Geophysical Research Letters

RESEARCH LETTER
10.1029/2023GL105819

Climate-Driven Fluctuations in Anthropogenic CO_2 Uptake by the East Sea in the North Pacific Ocean

So-Yun Kim[1], Kitack Lee[2], Tongsup Lee[1], Ja-Myung Kim[2], and In-Seong Han[3]

[1]Department of Oceanography, Pusan National University, Busan, Korea, [2]Division of Environmental Science and Engineering, Pohang University of Science and Technology, Pohang, Korea, [3]Ocean Climate and Ecology Research Division, National Institute of Fisheries Science, Busan, Korea

Key Points:

- The rate of anthropogenic CO_2 increase in the East Sea showed cyclic trends
- The cyclic trends of anthropogenic CO_2 increase were linked to the Arctic Oscillation
- Our findings shed light on changes in anthropogenic CO_2 uptake and transport by the global ocean in response to climate variations

Supporting Information:

Supporting Information may be found in the online version of this article.

Correspondence to:

K. Lee and T. Lee,
ktl@postech.ac.kr;
tlee@pusan.ac.kr

Citation:

Kim, S.-Y., Lee, K., Lee, T., Kim, J.-M., & Han, I.-S. (2023). Climate-driven fluctuations in anthropogenic CO_2 uptake by the East Sea in the North Pacific Ocean. *Geophysical Research Letters*, *50*, e2023GL105819. https://doi.org/10.1029/2023GL105819

Received 9 AUG 2023
Accepted 20 OCT 2023

Author Contributions:

Conceptualization: Kitack Lee, Tongsup Lee
Data curation: So-Yun Kim, Kitack Lee, Tongsup Lee
Investigation: So-Yun Kim, In-Seong Han
Methodology: Kitack Lee, Tongsup Lee
Supervision: Kitack Lee, Tongsup Lee
Validation: Kitack Lee, Tongsup Lee
Visualization: So-Yun Kim, Ja-Myung Kim
Writing – original draft: So-Yun Kim, Kitack Lee

Abstract Ocean ventilation is a key mechanism for transporting anthropogenic CO_2 (C^{ANTH}) from the ocean surface toward its interior. We investigated the link between ocean ventilation and C^{ANTH} increase in the East Sea using data from surveys conducted in 1992, 1999, 2007, and 2019. Between 1992 and 1999, the East Sea Intermediate Water (300−1,500 m) accumulated C^{ANTH} at a rate of 0.3 ± 0.1 mol C m^{-2} yr^{-1}. However, in the subsequent period (1999−2007) this rate decreased to <0.1 ± 0.1 mol C m^{-2} yr^{-1}. There was a resurgence in the C^{ANTH} increase rate between 2007 and 2019, reaching 0.4 ± 0.1 mol C m^{-2} yr^{-1}. The East Sea Intermediate Water ventilation changes, inferred from the changes in water column O_2 level and the Arctic Oscillation-driven winter surface temperature in the deep water formation region, were responsible for the periodic decline and recovery in C^{ANTH} increase.

Plain Language Summary Ocean ventilation plays a crucial role in transporting anthropogenic CO_2 from the surface toward the deep ocean interior. In the East Sea, demonstrating a direct causal relationship between ocean ventilation and anthropogenic CO_2 uptake has remained elusive because of limited observational evidence. To address this knowledge gap, we conducted direct measurements of carbon parameters during four surveys in the East Sea that together spanned nearly three decades (1992, 1999, 2007, and 2019). Our investigation revealed a cyclical pattern of waxing and waning in the rate of anthropogenic CO_2 increase within the East Sea over the past three decades. Significantly, we demonstrated that fluctuations in the ventilation of the East Sea were the primary driving force behind the decadal changes in anthropogenic CO_2 increase. Furthermore, our research unveiled a potential connection between the periodic fluctuations in surface temperature linked to the Arctic Oscillation and variations in East Sea ventilation. Our findings shed light on the intricate dynamics between ocean ventilation, winter sea surface temperature patterns, and CO_2 uptake in the East Sea.

1. Introduction

Since the onset of the Industrial Revolution approximately half of the anthropogenic CO_2 (C^{ANTH}) emissions resulting from human activities, including fossil fuel combustion, land use alterations, and cement production, have persisted in the Earth's atmosphere. The remaining portion has been absorbed by the world's oceans and terrestrial ecosystems (Friedlingstein et al., 2022; Gruber et al., 2019; Sabine et al., 2004). The potential for C^{ANTH} storage within the global ocean is significant, as the ocean already contains 40 times more carbon than the atmosphere (Canadell et al., 2021).

It is known that vertical ocean ventilation is crucial for effectively transporting C^{ANTH} from the surface to the deeper layers of the ocean, which ultimately affects the ocean's ability to absorb C^{ANTH}. However, a definitive cause-and-effect relationship between the intensity of ocean ventilation and the rate of C^{ANTH} change remains challenging (Lee et al., 2011), primarily because of the limited availability of multi-decadal data for most ocean regions. Previous studies have reported that C^{ANTH} has reached the ocean bottom in the East Sea, with concentrations in the deep waters exceeding detection limits by a slight margin (Park et al., 2006, 2008). These findings suggest that ocean ventilation could contribute to the amount of C^{ANTH} added to the water column. However, these studies did not provide observational evidence to substantiate their hypothesis.

Three key factors make the East Sea ideal for assessing how the oceanic increase of C^{ANTH} responds to changes in ocean ventilation intensity (Lee et al., 2011). First and foremost, the East Sea has an ocean ventilation system that operates on short time scales (decades to centuries) (Gamo et al., 2001; Kim & Kim, 1996; Yoon et al., 2018).

Writing – review & editing: So-Yun Kim, Kitack Lee, Tongsup Lee, Ja-Myung Kim, In-Seong Han

Second, the East Sea interior receives C^{ANTH}-enriched surface waters primarily from its northern basin, and these waters do not flow out into the adjacent North Pacific Ocean. Consequently, the basin acts as reservoir, retaining nearly all the C^{ANTH} absorbed by the East Sea. Lastly, the availability of multi-decadal data sets for the East Sea provides the necessary foundation for testing our hypothesis regarding the relationship between ocean ventilation intensity and C^{ANTH} increase.

The ventilation process in the East Sea, which is responsible for transporting salts, heat, and dissolved gases from the surface to the ocean interior, is closely associated with the formation of intermediate and deep waters. This ventilation is influenced by two environmental drivers that work together synergistically. The primary driver is a subtle density gradient that occurs with depth, resulting in a weak stability of the water column (Kim & Kim, 1996; Kim et al., 2001). This facilitates effective ventilation in the East Sea, in response to even minor surface perturbations. The second driver is the frequent formation of cold and dense surface water associated with variations in the Arctic Oscillation (AO) (Cui & Senjyu, 2010; Nam et al., 2016; Park, 2022). These climate-driven changes in ventilation intensity can either diminish or enhance the transfer of C^{ANTH}-enriched surface water to the basin interior (Min & Warner, 2005; Park et al., 2006). Over the past three decades, the ventilation intensity in the East Sea has changed, resulting in corresponding alterations in the O_2, nutrient, and probably C^{ANTH} concentrations within the Intermediate Water (Chen et al., 2017; Na et al., 2022).

In this study, we quantified the amount of C^{ANTH} that accumulated over three distinct time periods (1992−1999, 1999−2007, and 2007−2019) within the East Sea. We employed an extended multiple linear regression approach using data sets collected in 1992, 1999, 2007, and 2019. This method enabled calculation of the rates of C^{ANTH} increase across three decades involved. Moreover, we conducted a comparative analysis of the rates of C^{ANTH} increase and the changes in the O_2 concentration in the East Sea Intermediate Water. This comparison aimed at determining whether changes in ventilation intensity directly contributed to changes in C^{ANTH} increase. This study stands out for its focus on quantifying C^{ANTH} increase over specific time periods, in contrast to previous research mainly centered on assessing the distributions of C^{ANTH} and C_T (Chen et al., 1995; Na et al., 2022; Park et al., 2006). Additionally, it provides confirmation of a direct connection between decadal changes in the C^{ANTH} and variations in the East Sea ventilation, primarily driven by the AO.

2. Data and Methods

2.1. Data Collection and Evaluation of Data Consistency

The analytical methods used for measuring seawater carbonate parameters, including total dissolved inorganic carbon ($C_T = [CO_2] + [HCO_3^-] + [CO_3^{2-}]$) and total alkalinity ($A_T \approx [HCO_3^-] + 2[CO_3^{2-}] + [B(OH)_4^-] + [OH^-] - [H^+]$), during the 1992, 1999, and 2007 studies have been documented by Chen et al. (1995), Talley et al. (2004), and Park et al. (2008), respectively.

For the 2019 data collection, samples were obtained from 32 hydrographic stations aboard the Russia research vessel R/V Akademik Oparin, conducted from 27 October to 22 November 2019 (Figure 1e). At all 32 stations, seawater samples were collected to measure basic water properties, such as salinity, temperature, oxygen, and nutrients, spanning from the surface to depths of 3,600 m. The dissolved oxygen and nutrients concentrations were determined using an automated oxygen titrator based on the Winkler method and a continuous flow analyzer, respectively (Talley et al., 2004). Additionally, at 22 selected stations, seawater samples were collected for C_T and A_T measurements, covering the same depth range. The C_T and A_T concentrations were measured using a VINDTA system, which utilizes both coulometric titration and potentiometric titration methods (manufactured by Marianda, Kiel, Germany). The accuracy of the C_T and A_T measurements was assessed by comparing the daily titration results obtained for seawater reference materials with their certified C_T and A_T values. These reference materials and certified C_T and A_T values were provided by A. Dickson of Scripps Institution of Oceanography, USA. Across all analysis periods, the measurement accuracy for C_T and A_T was determined to be ±2 μmol kg^{-1}, based on onboard analysis using the certified reference materials.

During our cruises we observed slight deviations in the measured values of A_T (ranged from −2.4 to +2.8 μmol kg^{-1}) and C_T (−1.5 to +2.5 μmol kg^{-1}) when compared with the certified values of the reference materials. To account for these observed deviations, we either added or subtracted the deviations from the values obtained from seawater samples collected during the same period when the reference materials were analyzed. These deviations were attributed to instability or drift in the performance of the coulometry method used for C_T

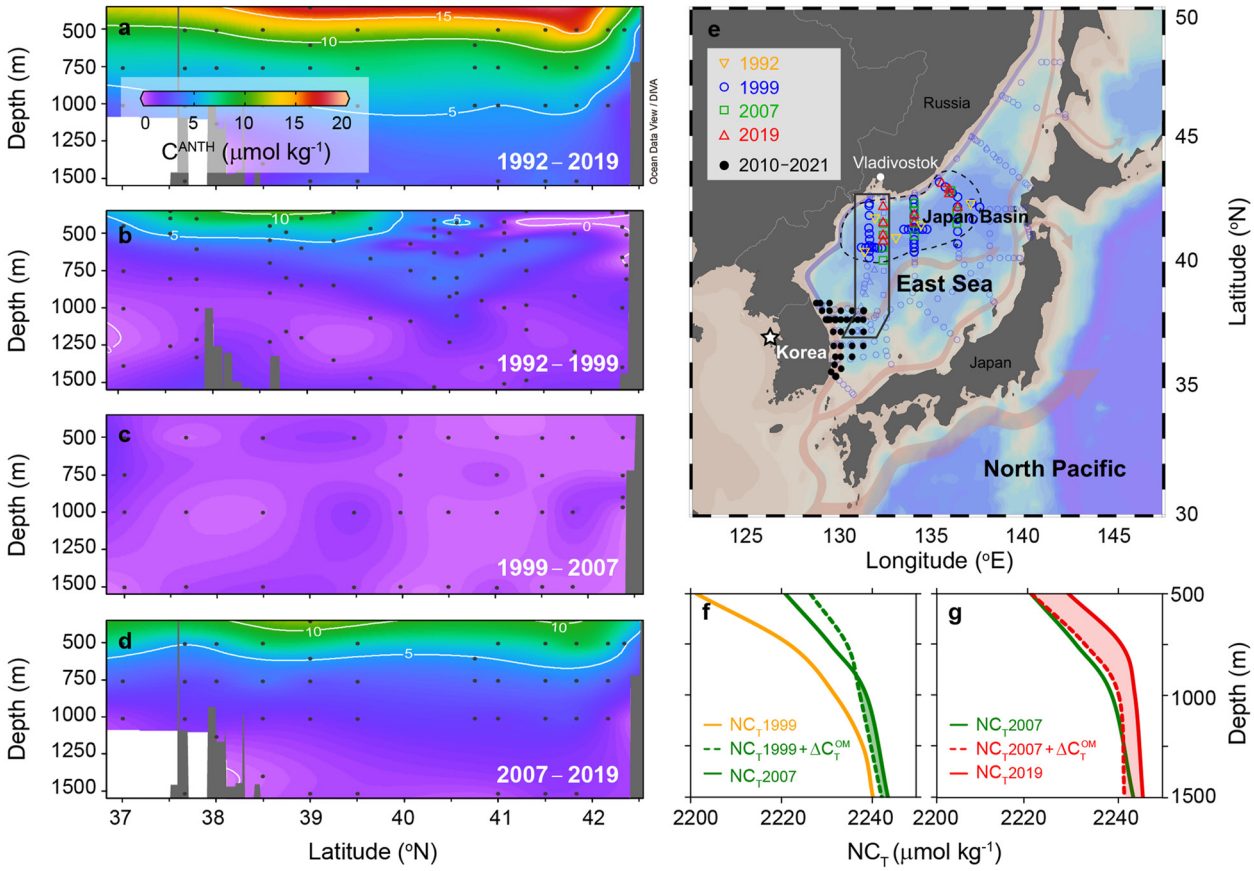

Figure 1. Meridional distributions of C^{ANTH} accumulated in the East Sea from 37°N to 42.5°N during the periods (a) 1992–2019, (b) 1992–1999, (c) 1999–2007, and (d) 2007–2019. The solid line area in (e) indicates the sampling locations for calculating C^{ANTH} increase. (e) All sampling locations in the East Sea during the period 1992–2021. The East Sea interacts with the North Pacific Ocean to the east and East China Sea to the southwest solely through three shallow straits with depths of less than 150 m. Open symbols indicate the hydrographic stations for the cruises conducted in 1992–2019. C_T and A_T samples in the Japan basin (within the dashed line; data used in Figure 2) were collected in 1992 (yellow reverse triangles), 1999 (blue circles), 2007 (green squares), and 2019 (red triangles). The seasonal cruises (solid black circles) were carried out along the east coast of Korea after 2010 (data used in Figure 3). The star on the west coast of Korea marks the atmospheric pCO_2 monitoring site, Anmyun-do. The pathways of warm (red) and cold (blue) surface currents are adapted from Park et al. (2019). (f, g) The vertical mean profiles of NC_T ($NC_T = C_T \times 34.07/S$; 34.07 was chosen as the mean salinity of the deep waters) for the Japan Basin, within the dashed line in (e), were acquired during the 1999 (yellow solid line), 2007 (green solid line), 2019 (red solid line) cruises. Estimated NC_T profiles, which reflect only the organic matter oxidation effects (=Δ[P] × C:P + initial [NC_T]), were obtained for 2007 (green dotted line) and 2019 (red dotted line), respectively.

measurement and a glass electrode utilized for A_T measurement. This practice of adjusting data is necessary when comparing data sets collected in different years, as it helps ensure the consistency and accuracy of the measurements by accounting for any instrument performance variations over time.

Data comparison was made to assess for the presence of any systematic differences among the data sets. Because the 1999 data set had the most extensive coverage in terms of the number of sampling stations involved and parameters measured (open circles in Figure 1e), it was selected as the reference data set for comparison. The comparison was made as a function of seawater density below 2,000 m in the East Sea Japan Basin. Tsunogai et al. (1993) and Kim et al. (2001) estimated the turnover time of the Japan Basin deep waters to be approximately 100 years. Therefore, when comparing the various data sets for waters deeper than 2,000 m, any observed differences were attributed to systematic measurement errors. The differences observed among the data sets are summarized in Text S1 and Table S1 (also Figure S1 in Supporting Information S1). Based on the mean differences identified, adjustments were made to the data sets for 1992, 2007, and 2019. The resulting data sets were internally consistent to ±0.004°C for temperature, ±0.001 for salinity, ±1 μmol kg^{-1} for oxygen, ±0.1 μM for nitrate, ±0.01 μM for phosphate, ±0.6 μM for silicate, and ±2 μmol kg^{-1} for C_T and A_T.

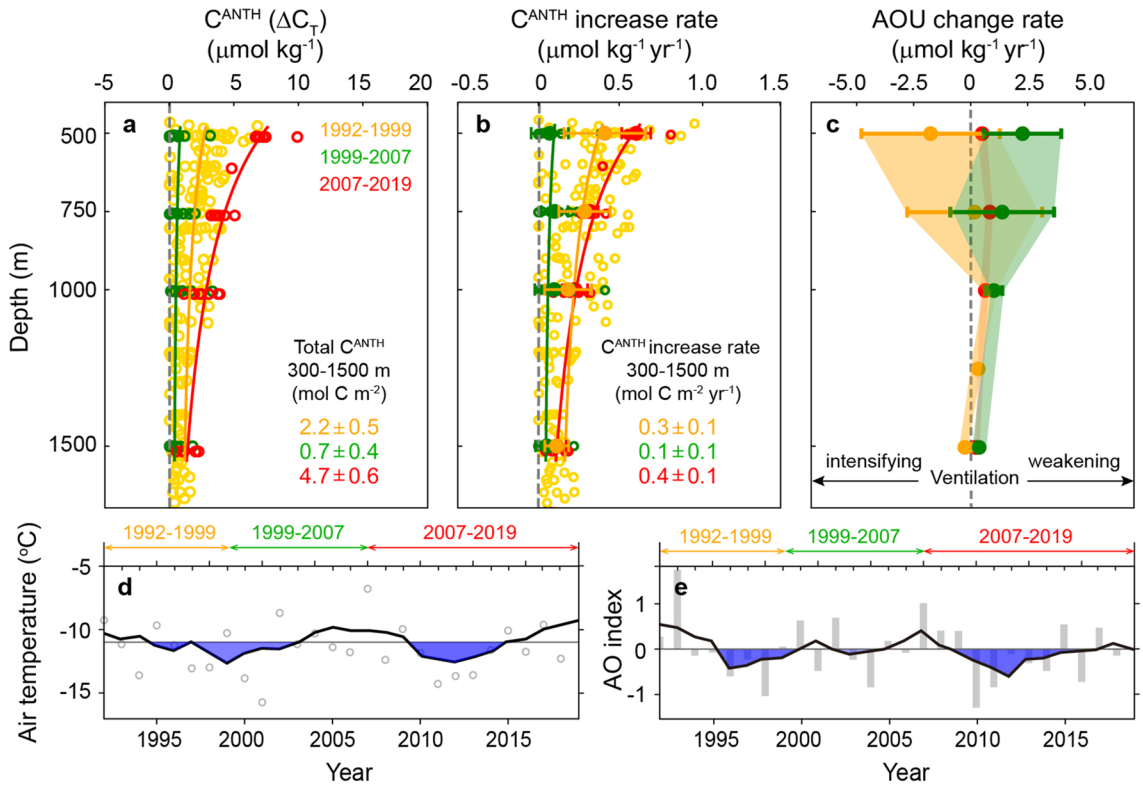

Figure 2. Vertical profiles of (a) C^{ANTH} ($\Delta C_T = C_T^{(t+1)} - C_T^{(t)}$), (b) rates of C^{ANTH} increase, and (c) rates of AOU change below 300 m for the periods 1992−1999 (yellow circles and lines), 1999−2007 (green circles and lines), and 2007−2019 (red circles and lines). The solid circles and error bars in (b, c) indicate mean values and one standard deviation from the mean, respectively, obtained from all data collected within 50 m above and below 500, 750, 1,000, and 1,500 m. Variations in (d) air temperature (January mean) and (e) AO index (5-year moving average) in January at Vladivostok from 1992 to 2019. The horizontal solid line in (d) indicates the mean value of air temperature (−11°C) during the period.

2.2. C^{ANTH} Accumulation in Waters Deeper Than 300 m

The extended Multi-Linear Regression (eMLR) method, accounting for all the variations in seawater C_T while isolating the C^{ANTH} component for estimation (Friis et al., 2005), is a useful approach for estimating the increase in C_T between data sets obtained in different years ($C^{ANTH} = C_T^{(t+1)} - C_T^{(t)}$). Over time, the initial eMLR method has undergone improvements in terms of reliability, and we used a refined version (Carter et al., 2019; Clement & Gruber, 2018; Gao et al., 2022; Gruber et al., 2019; Plancherel et al., 2013). The key to the eMLR method lies in the selection of predictors used in the regression process, as this choice significantly affects the accuracy of C^{ANTH} results. To determine the C^{ANTH} concentration in the East Sea Intermediate Water, we considered 21 combinations of predictors within the eMLR framework. After assessing the performance of the combinations, we ultimately chose the five eMLR functionalities that yielded the smallest root mean square errors (RMSEs) or residuals (Text S2 and Table S2 in Supporting Information S1).

We fitted each of the 1999, 2007, and 2019 data sets to six variables that were shown to best explain C_T variations, including θ (potential temperature), salinity, AOU (apparent oxygen utilization), A_T, silicate, and phosphate. To include the 1992 data set (which included no nutrient data) in the eMLR, we fitted each of the 1992 and 1999 C_T data sets to only four predictor variables (θ, salinity, AOU, and A_T). The choice of the five MLR functionalities had a negligible impact on the differences between the measured and predicted C_T (see Text S3 and Table S5 in Supporting Information S1).

The C^{ANTH} concentration reported in our study is subject to various sources of error, including measurement errors, uncertainties related to the choice of the eMLR method, and uncertainties associated with the depth range for which the eMLR was derived. To quantify the overall uncertainty in the C^{ANTH} concentration, we calculated the square root of the sum of the squares of the uncertainties from the sources of error mentioned above. As a

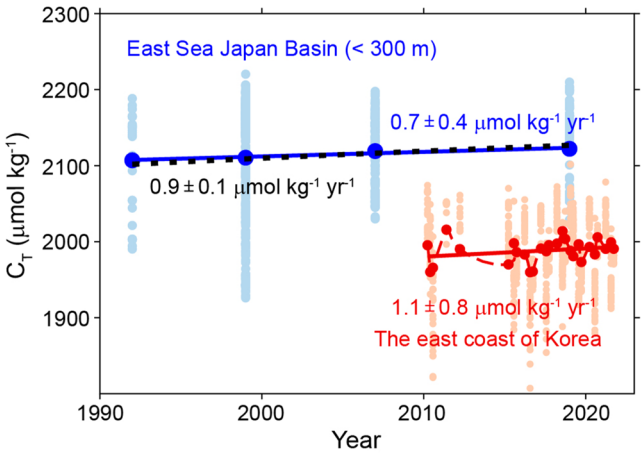

Figure 3. The rate of annual increase in C_T (C^{ANTH}) in the surface mixed layer for the Japan Basin during 1992–2019 (blue solid circles and line) and along the east coast of Korea at 2010−2021 (red solid circles and line). The dotted line represents the predicted rate of C_T (C^{ANTH}) increase, which was calculated from A_T value of 2,264.2 μmol kg^{-1} (at salinity of 33.97) and surface pCO_2 values using the carbonic acid dissociation constants of Mehrbach et al. (1973), as refitted by Dickson and Millero (1987), assuming that surface pCO_2 follows the increase in atmospheric pCO_2. The A_T value used in this calculation may have included small contributions from dissolved organic matter (Ko et al., 2016) and phytoplankton and bacteria cells (Lee et al., 2021). However, as long as these organic contributions to A_T exhibited a consistent trend during the study period, they did not impact the predicted rate of surface C_T.

result of this analysis, the uncertainty in the C^{ANTH} concentration was determined to be 3.1–3.8 μmol kg^{-1} for all three periods examined (detailed in Text S3 in Supporting Information S1).

2.3. C^{ANTH} Accumulation Within 300 m Depth

To determine the rate of surface C^{ANTH} increase during the study period from spanning 1992 to 2019, we applied linear regression to all C_T data acquired from four surveys conducted in the northern basin of the East Sea. To validate the resulting rate, we also cross-checked our finding using additional C_T data set from Kim et al. (2020) collected from the coast of Korea for the period 2010 to 2021 (solid circles in Figure 1e). For all of our analyses, we considered data from the maximum winter mixed layer, which extended to a depth of 300 m. This depth was determined based on seawater density gradients (Lim et al., 2012).

2.4. Arctic Oscillation (AO) Index and Air Temperature Over Vladivostok

AO index data were provided by the Climate Prediction Center, National Oceanic and Atmospheric Administration, USA. The daily AO index is constructed by projecting the daily 1,000 mb height anomalies poleward of 20°N onto the loading pattern of the AO. The loading pattern of the AO is defined as the leading mode of Empirical Orthogonal Function (EOF) analysis of monthly mean 1,000 mb height during the period 1979−2000.

Also, we incorporated reanalyzed air temperature data (a resolution of 0.25° × 0.25°) obtained from the European Centre for Medium-Range Weather Forecasts Reanalysis version 5 on single levels from 1940 to present (Hersbach et al., 2023). We used the monthly mean air temperature data for the period 1990−2021 in Vladivostok.

3. Results

3.1. C^{ANTH} in Deep Waters (Deeper Than 300 m)

During the three decades (1992−2019), most of the C^{ANTH} that entered the East Sea Japan Basin accumulated in the water depths of 300–1,500 m, which includes the East Sea Intermediate Water (Figures 1a–1d). Below 1,500 m, the C^{ANTH} was found to be almost absent (Text S4 and Figure S6 in Supporting Information S1). The amount of accumulated C^{ANTH} was greater in waters close to the base of the winter mixed layer (nominally 300 m), but rapidly decreased approaching the lower boundary of the Intermediate Water (Figures 1a–1d and 2a). The most striking feature was that the rate of increase in C^{ANTH} varied markedly over decadal time scales (Figure 2b). At 500 m depth, the rate of increase in C^{ANTH} was 0.4 ± 0.3 μmol kg^{-1} yr^{-1} for the earliest period (1992−1999). However, in the subsequent period (1999−2007) C^{ANTH} increase decreased considerably (0.1 ± 0.1 μmol kg^{-1} yr^{-1}). Remarkably, the rate of increase observed in the latest period of the study (2007−2019) was 0.6 ± 0.1 μmol kg^{-1} yr^{-1}, indicating that the rate of CO_2 increase returned to a level similar to or higher than that in the earliest period. The rates of increase in C^{ANTH} in both the earliest and latest periods decreased rapidly with increasing depth. However, for the intervening period (1999−2007), we found almost no increase in C^{ANTH} throughout the water column (green circles in Figures 2a and 2b).

The total C^{ANTH} that accumulated in the water column (300−1,500 m depth; per m^2) in the period 1999−2007 was close to zero; however, both the earliest and most recent periods yielded considerably higher values: 2.2 ± 0.5 mol C m^{-2} (0.3 ± 0.1 mol C m^{-2} yr^{-1}) and 4.7 ± 0.6 mol C m^{-2} (0.4 ± 0.1 mol C m^{-2} yr^{-1}), respectively (Figures 2a and 2b). Thus, the degree of transport of C^{ANTH} to the Japan Basin interior varied considerably, ranging from being strong in the period 1992−1999, to substantially less in the period 1999−2007, then returning to strongest in the period 2007−2019.

3.2. C^{ANTH} in the Surface Ocean (Shallower Than 300 m)

In contrast to the rates of increase in C^{ANTH} observed in the East Sea Intermediate Water, the rate of C_T increase in the surface mixed layer remained relatively consistent, at 0.7 ± 0.4 μmol kg^{-1} yr^{-1}, over the period from 1992 to 2019 (Figure 3). The observed rate likely comprised contributions from anthropogenic and natural factors. We found only minor changes in surface properties of the northern basin throughout the study period, including for A_T (2,264.2 ± 2.5 μmol kg^{-1}), salinity (33.97 ± 0.04), phosphate (0.7 ± 0.1 μM), nitrate (9.1 ± 0.7 μM). Therefore, it is less likely that the observed rate of C_T increase can be attributed to the possible intrusion of C_T-rich water (natural component). Consequently, the measured rate predominantly reflects the C^{ANTH} component.

The determined rates of the surface C^{ANTH} increase for the northern basin (0.7 ± 0.4 μmol kg^{-1} yr^{-1}) and the East Sea coastal waters (1.1 ± 0.8 μmol kg^{-1} yr^{-1}) agree with the rate of 0.9 ± 0.1 μmol kg^{-1} yr^{-1} predicted based on atmospheric CO_2 increase (Figure 3). These three estimates are essentially indistinguishable when considering the uncertainties involved in each calculation. The agreement between the two observed and predicted rates suggests that the increase in C_T in the surface of the East Sea is indeed in step with the rise in atmospheric CO_2, a trend that has also been observed in other ocean basins (Carter et al., 2017; Gao et al., 2022).

4. Discussions

4.1. Causes of C^{ANTH} Accumulation Changes

The accumulation of C^{ANTH} in the East Sea Japan Basin underwent a marked reduction between 1992−1999 and 1999−2007, but this accumulation subsequently reversed in 2007–2019. These fluctuations likely stemmed from variations in the ventilation of the East Sea Intermediate Water, especially within the water masses ranging from 300 to 1,500 m. These water masses contained nearly all of the accumulated C^{ANTH} between 1992 and 2019. To gain insights into changes in ventilation intensity, one can examine changes in the O_2 concentration of the Intermediate Water. This approach assumes that the amount of O_2 consumed in the oxidation of organic matter settling from the surface did not change over the study period. This diagnostic mechanism has been used in previous studies, which have shown that reductions in the O_2 concentration in the ocean interior are primarily influenced by changes in water column ventilation, rather than changes in the rate of O_2 demand for organic matter oxidation (Deutsch et al., 2006; Joos et al., 2003; Kim et al., 2010; McDonagh et al., 2005).

Values for AOU (=the saturated [O_2] − the measured [O_2]) provided the valuable insights into the state of the East Sea Intermediate Water. Under conditions of weakening ventilation, bacterial consumption of O_2 for organic matter oxidation surpasses the supply of O_2 through the isopycnal transport of waters from the formation site to the observation point. This leads to an increase in the AOU of the Intermediate Water. Conversely, in cases of active ventilation, the supply of O_2 from the surface exceeds O_2 consumption, resulting in a decrease in the AOU throughout the water column. The trend of AOU values observed during 1999–2007 (green circles in Figure 2c) was consistent with weakening ventilation, whereas the trends for 1992−1999 (yellow circles in Figure 2c) and 2007−2019 (red circles in Figure 2c) were consistent with active ventilation. When taking into account the magnitudes of the errors, the rates of AOU increase for both the earliest and latest periods were practically indistinguishable.

We also found the similar trends in the annual rates of AOU change and C^{ANTH} increase within the East Sea Intermediate Water (Figures 2b vs. 2c). These findings highlight the strong connection between the declining AOU rates and the increasing C^{ANTH} rates in the East Sea Intermediate Water. This compelling evidence underscores that the temporal change in the ventilation intensity of the Intermediate Water was a primary driving factor behind the waxing and waning of C^{ANTH} accumulation in this region.

In addition to our AOU data, we supplemented our assessment of ventilation intensity with air temperature data from Vladivostok, a location in close proximity to the deep water formation region. We specifically focused on the month of January, known for its significant deep water formation activity. The analysis of air temperature data also revealed that the ventilation intensity during the earliest and latest periods was similar, but considerably stronger than during the intervening period (Figure 2d), as discussed in the next section. Winter surface water properties including temperature and salinity in the northern basin of the East Sea are directly influenced by the winter air temperature in the vicinity of Vladivostok. These variations in air temperature respond to variations in the AO index (Cui & Senjyu, 2010; Nam et al., 2016; Tanaka, 2014). During negative phases of the AO index,

cold Arctic air advances southward, producing strong winds over Vladivostok. The resulting large drop in air temperature increases the surface water density in the northern basin, making it similar to that of the Intermediate Water and facilitating its ventilation. Conversely, during positive AO phases, when the cold Arctic air retreats with less severe temperature drops, the ventilation of the Intermediate Water tends to decrease. These atmospheric influences help explain the observed changes in ventilation intensity in the East Sea.

Our conclusion is further substantiated by the results of analysis of the water column phosphate and salinity-normalized C_T (NC_T) (Figures 1f and 1g). Specifically, for 1999−2007, the increase in NC_T resulting from organic matter oxidation (calculated by multiplying Δ[P] by the C:P ratio of 117, as described by Anderson and Sarmiento (1994)) entirely accounted for the NC_T differences observed between 1999 and 2007 (compare the green dotted and solid lines in Figure 1f). However, for the period 2007−2019, the increase in NC_T resulting from organic matter oxidation only explained 20% of the C_T differences observed between 2007 and 2019 (compare the red dotted and solid lines in Figure 1g). These findings suggest that the supply of C^{ANTH}-rich surface water to the Intermediate Water through ventilation was negligible in the period 1999−2007, but substantial in the period 2007−2019.

4.2. Cause of Ventilation Changes in the East Sea Intermediate Water

In our analysis, we used the AO index values for January because January corresponds to the predominant period of deep water formation near Vladivostok, when air temperatures are lowest during the year (Talley et al., 2003). The mean AO index values for January did not show significant differences among the three study periods. However, we observed more pronounced negative AO index values during the earliest (1992−1999) and latest (2007−2019) periods (the blue shades in Figure 2e). In contrast, the negative values were less pronounced during the intervening period (1999−2007). Thus, the January AO index values appeared to be synchronized with the patterns of waxing and waning of C^{ANTH} accumulation in the Intermediate Water (Figures 2a and 2b). This suggests a compelling link between the AO-driven variations in ocean ventilation and the decadal fluctuations of C^{ANTH} increase in the Intermediate Water.

Occasional deep ventilation events could have affected our general conclusion. It has been reported that in the cold winter during the 2000−2001 transition, dense surface water sank to depths greater than that of the Intermediate Water (Kim et al., 2001), potentially transporting C^{ANTH} to depths deeper than the lower limit of the Intermediate Water. However, despite the occurrence of such isolated events, we did not observe discernible C^{ANTH} signals in the deep waters during the 1992−2019 period. This suggests that infrequent deep ventilation events are unlikely to have influenced our general conclusion, regarding the primary drivers of C^{ANTH} increase in the Intermediate Water.

5. Conclusions and Implications

Extensive ocean and atmospheric observations over three decades enabled identification of a cyclical trend in the rate of C^{ANTH} increase in the East Sea. This involved an upturn in accumulation during the period 1992−1999, followed by a downturn from 1999 to 2007, and another upturn from 2007 to 2019. Our findings have strongly affirmed that changes in ventilation of the East Sea Intermediate Water, driven by the AO, are a primary driver behind the decadal changes in the rate of CO_2 increase in the East Sea.

As the East Sea experiences a progressive warming, the frequency and intensity of the Intermediate Water ventilation may decrease in the future. This weakening in ventilation will result in a lower rate of C^{ANTH} increase within the basin. The observed cause-and-effect association between ventilation intensity and C^{ANTH} increase rate in the East Sea is likely to also become increasingly evident in other major ocean basins, as consequence of global climate change.

Data Availability Statement

The monthly mean Arctic Oscillation index data since January 1950 are available from www.cpc.ncep.noaa.gov/products/precip/CWlink/daily_ao_index/ao.shtml. The air temperature of ERA5 hourly data on single levels from 1940 to present was obtained from Hersbach et al. (2023). The atmospheric pCO_2 measured at Anmyun-do

(Korean coast of the Yellow Sea) data was downloaded from www.climate.go.kr/home/09_monitoring/search/search. The data sets presented in this paper are available in the online data repository (Lee & Lee, 2023).

Acknowledgments
Our profound appreciation goes to three reviewers for their thorough and insightful comments, which have greatly improved the paper's quality in methodology, error analysis, and data interpretation. This study was supported by the National Research Foundation (NRF) of Korea (NRF-2021M316A1089658 for the Carbon Cycle between Oceans, Land, and Atmosphere) and the National Institute of Fisheries Science, Ministry of Oceans and Fisheries (R2023044).

References

Anderson, L. A., & Sarmiento, J. L. (1994). Redfield ratios of remineralization determined by nutrient data analysis. *Global Biogeochemical Cycles*, *8*(1), 65–80. https://doi.org/10.1029/93GB03318

Canadell, J. G., Monterio, P. M. S., Costa, M. H., Cotrim da Cunha, L., Cox, P. M., Eliseev, A. V., et al. (2021). Global carbon and other biogeochemical cycles and feedbacks. In V. Masson-Delmott, et al. (Eds.), *Climate change 2021: The physical science basis, contribution of working Group I to the sixth assessment report of the intergovernmental panel on climate change* (pp. 673–816). Cambridge University Press. https://doi.org/10.1017/9781009157896.007

Carter, B. R., Feely, R. A., Mecking, S., Cross, J. N., Macdonald, A. M., Siedlecki, S. A., et al. (2017). Two decades of Pacific anthropogenic carbon storage and ocean acidification along global ocean ship-based hydrographic investigations program section P16 and P02. *Global Biogeochemical Cycles*, *31*(2), 306–327. https://doi.org/10.1002/2016GB005485

Carter, B. R., Feely, R. A., Wanninkhof, R., Kouketsu, S., Sonnerup, R. E., Pardo, P. C., et al. (2019). Pacific anthropogenic carbon between 1991 and 2017. *Global Biogeochemical Cycles*, *33*(5), 597–617. https://doi.org/10.1029/2018GB006154

Chen, C.-T. A., Lui, H.-K., Hsieh, C.-H., Yanagi, T., Kosugi, N., Ishii, M., & Gong, G.-C. (2017). Deep oceans may acidify faster than anticipated due to global warming. *Nature Climate Change*, *7*(12), 890–894. https://doi.org/10.1038/s41558-017-0003-y

Chen, C.-T. A., Wang, S. L., & Bychkov, A. S. (1995). Carbonate chemistry of the Sea of Japan. *Journal of Geophysical Research*, *100*(C7), 13737–13745. https://doi.org/10.1029/95JC00939

Clement, D., & Gruber, N. (2018). The eMLR (C*) method to determine decadal changes in the global ocean storage of anthropogenic CO_2. *Global Biogeochemical Cycles*, *32*(4), 654–679. https://doi.org/10.1002/2017GB005819

Cui, Y. L., & Senjyu, T. (2010). Interdecadal oscillations in the Japan Sea proper water related to Arctic Oscillation. *Journal of Oceanography*, *66*(3), 337–348. https://doi.org/10.1007/s10872-010-0030-z

Deutsch, C., Emerson, S., & Thompson, L. (2006). Physical-biological interactions in North Pacific oxygen variability. *Journal of Geophysical Research*, *111*(C9), C09S90. https://doi.org/10.1029/2005JC003179

Dickson, A. G., & Millero, F. J. (1987). A comparison of the equilibrium constants for the dissociation of carbonic acid in seawater media. *Deep-Sea Research, Part A: Oceanographic Research Papers I*, *34*(10), 1733–1743. https://doi.org/10.1016/0198-0149(87)90021-5

Friedlingstein, P., O'Sullivan, M., Jones, M. W., Andrew, R. M., Gregor, L., Hauck, J., et al. (2022). Global carbon budget 2022. *Earth System Science Data*, *14*(11), 4811–4900. https://doi.org/10.5194/essd-14-4811-2022

Friis, K., Körtzinger, A., Pätsch, J., & Wallace, D. W. (2005). On the temporal increase of anthropogenic CO_2 in the subpolar North Atlantic. *Deep-Sea Research, Part A: Oceanographic Research Papers I*, *52*(5), 681–698. https://doi.org/10.1016/j.dsr.2004.11.017

Gamo, T., Momoshima, N., & Tolmachyov, S. (2001). Recent upward shift of the deep convection system in the Japan Sea, as inferred from the geochemical tracers tritium, oxygen, and nutrients. *Geophysical Research Letters*, *28*(21), 4143–4146. https://doi.org/10.1029/2001GL013367

Gao, H., Cai, W.-J., Jin, M., Dong, C., & Timmerman, A. H. V. (2022). Ocean ventilation controls the contrasting anthropogenic CO_2 uptake between the western and eastern South Atlantic Ocean basins. *Global Biogeochemical Cycles*, *36*(6), e2021GB007265. https://doi.org/10.1029/2021GB007265

Gruber, N., Clement, D., Carter, B. R., Feely, R. A., Van Heuven, S., Hoppema, M., et al. (2019). The oceanic sink for anthropogenic CO_2 from 1994 to 2007. *Science*, *363*(6432), 1193–1199. https://doi.org/10.1126/science.aau5153

Hersbach, H., Bell, B., Berrisford, P., Biavati, G., Horányi, A., Muñoz Sabater, J., et al. (2023). ERA5 hourly data on single levels from 1940 to present [Dataset]. Copernicus Climate Change Service (C3S) Climate Data Store (CDS). https://doi.org/10.24381/cds.adbb2d47

Joos, F., Plattner, G.-K., Stocker, T. F., Körtzinger, A., & Wallace, D. W. R. (2003). Trends in marine dissolved oxygen: Implications for ocean circulation changes and the carbon budget. *Eos Trans. AGU*, *84*(21), 197–201. https://doi.org/10.1029/2003EO210001

Kim, J.-M., Lee, K., Han, I.-S., Lee, J.-S., Choi, Y.-H., Lee, J. H., & Moon, J. (2020). Anthropogenic nitrogen-induced changes in seasonal carbonate dynamics in a productive coastal environment. *Geophysical Research Letters*, *47*(17), e2020GL088232. https://doi.org/10.1029/2020GL088232

Kim, K., Kim, K.-R., Min, D.-H., Volkov, Y., Yoon, J.-H., & Takematsu, M. (2001). Warming and structural changes in the East (Japan) Sea: A clue to future changes in global oceans? *Geophysical Research Letters*, *28*(17), 3293–3296. https://doi.org/10.1029/2001GL013078

Kim, K.-R., & Kim, K. (1996). What is happening in the East Sea (Japan Sea): Recent chemical observations during CREAMS 96-96. *Journal of the Korean Society of Oceanography*, *31*, 164–172. https://doi.org/10.7850/jkso.2014.19.4.287

Kim, T.-W., Lee, K., Feely, R. A., Sabine, C. L., Chen, C.-T. A., Jeong, H. J., & Kim, K. Y. (2010). Prediction of Sea of Japan (East Sea) acidification over the past 40 years using a multiparameter regression model. *Global Biogeochemical Cycles*, *24*(3), GB3005. https://doi.org/10.1029/2009GB003637

Ko, Y. H., Lee, K., Eom, K. H., & Han, I.-S. (2016). Organic alkalinity produced by phytoplankton an its effect on the computation of ocean carbon parameters. *Limnology & Oceanography*, *61*(4), 1462–1471. https://doi.org/10.1002/lno.10309

Lee, C.-H., Lee, K., Ko, Y. H., & Lee, J.-S. (2021). Contribution of marine phytoplankton and bacteria to alkalinity: An uncharacterized component. *Geophysical Research Letters*, *48*(19), e2021GL093738. https://doi.org/10.1029/2021GL093738

Lee, K., Chris, S., Tanhua, T., Kim, T.-W., Feely, R., & Kim, H.-C. (2011). Roles of marginal seas in absorbing and storing fossil fuel CO_2. *Energy & Environmental Science*, *4*, 1133–1146. https://doi.org/10.1039/C0EE00663G

Lee, K., & Lee, T. (2023). Anthropogenic CO_2 uptake by the East Sea (version 2) [Dataset]. Figshare. https://doi.org/10.6084/m9.figshare.24425140

Lim, S., Jang, C. J., Oh, I. S., & Park, J. (2012). Climatology of the mixed layer depth in the East/Japan Sea. *Journal of Marine Systems*, *96–97*, 1–14. https://doi.org/10.1016/j.jmarsys.2012.01.003

McDonagh, E. L., Bryden, H. L., King, B. A., Sanders, R. J., Cunningham, S. A., & Marsh, R. (2005). Decadal changes in the South Indian Ocean thermocline. *Journal of Climate*, *18*(10), 1575–1590. https://doi.org/10.1175/JCLI3350.1

Mehrbach, C., Cullberson, C. H., Hawley, J. E., & Pytkowicz, R. M. (1973). Measurement of the apparent dissociation constants of carbonic acid in seawater at atmospheric pressure. *Limnology & Oceanography*, *18*(6), 897–907. https://doi.org/10.4319/lo.1973.18.6.0897

Min, D. H., & Warner, M. J. (2005). Basin-wide circulation and ventilation study in the East Sea (Sea of Japan) using chlorofluoro-carbon tracers. *Deep-Sea Research Part II*, *52*(11–13), 1580–1616. https://doi.org/10.1016/j.dsr2.2003.11.003

Na, T., Hawng, J., Kim, S.-Y., Jeong, S., Rho, T. K., & Lee, T. (2022). Large increase in dissolved inorganic carbon in the East Sea (Japan Sea) from 1999 to 2019. *Frontiers in Marine Science*, *9*, 825206. https://doi.org/10.3389/fmars.2022.825206

Nam, S., Yoon, S.-T., Park, J.-H., Kim, Y. H., & Chang, K.-I. (2016). Distinct characteristics of the intermediate water observed off the east coast of Korea during two contrasting years. *Journal of Geophysical Research: Oceans*, *121*(7), 5050–5068. https://doi.org/10.1002/2015JC011593

Park, G.-H., Lee, K., & Tishchenko, P. (2008). Sudden, considerable reduction in recent uptake of anthropogenic CO_2 by the East/Japan Sea. *Geophysical Research Letters*, *35*(23), L23611. https://doi.org/10.1029/2008gl036118

Park, G. H., Lee, K., Tishchenko, P., Min, D. H., Warner, M. J., Talley, L. D., et al. (2006). Large Accumulation of anthropogenic CO_2 in the East (Japan) Sea and its significant impact on carbonate chemistry. *Global Biogeochemical Cycles*, *20*(4), 4013. https://doi.org/10.1029/2005GB002676

Park, J. J. (2022). Long-term variability of the East Sea Intermediate water thickness: Regime shift of intermediate layer in the mid-1990s. *Frontiers in Marine Science*, *9*, 923093. https://doi.org/10.3389/fmars.2022.923093

Park, K. A., Park, J. J., Park, J. E., Choi, B. J., Lee, S. H., Byun, D. S., et al. (2019). Interdisciplinary mathematics and sciences in schematic ocean current maps in the sea around Korea. In B. Sriraman (Ed.), *Handbook of the mathematics of the arts and sciences*. Springer. https://doi.org/10.1007/978-3-319-70658-0_37-1

Plancherel, Y., Rodgers, K. B., Key, R. M., Jacobson, A. R., & Sarmiento, J. L. (2013). Role of regression model selection and station distribution on the estimation of oceanic anthropogenic carbon change by eMLR. *Biogeosciences*, *10*(7), 4801–4831. https://doi.org/10.5194/bg-10-4801-2013

Sabine, C. L., Feely, R. A., Gruber, N., Key, R. M., Lee, K., Bullister, J. L., et al. (2004). The oceanic sink for anthropogenic CO_2. *Science*, *305*(5682), 367–371. https://doi.org/10.1126/science.1097403

Talley, L. D., Lobanov, S., Ponomarev, V., Salyuk, A., Tishchenko, P., Zhabin, I., & Rise, S. (2003). Deep convection and brine rejection in the Japan Sea. *Geophysical Research Letters*, *30*(4), 1159. https://doi.org/10.1029/2002GL016451

Talley, L. D., Tishchenko, P., Luchin, V., Nedashkovskiy, A., Sagalaev, S., Kang, D.-J., et al. (2004). Atlas of Japan (East) Sea hydrographic properties in summer, 1999. *Progress in Oceanography*, *61*(2–4), 277–348. https://doi.org/10.1016/j.pocean.2004.06.011

Tanaka, K. (2014). Formation of bottom water and its variability in the northwestern part of the Sea of Japan. *Journal of Geophysical Research: Oceans*, *119*(3), 2081–2094. https://doi.org/10.1002/2013JC009456

Tsunogai, S., Watanabe, Y. W., Harada, K., Watanabe, S., Saito, S., & Nakajima, M. (1993). Dynamics of the Japan Sea deep water studied with chemical and radiochemical tracers. *Elsevier Oceanography Series*, *59*, 105–119. https://doi.org/10.1016/S0422-9894(08)71321-7

Yoon, S.-T., Chang, K.-I., Nam, S., Rho, T., Kang, D.-J., Lee, T., et al. (2018). Re-initiation of bottom water formation in the East Sea (Japan Sea) in a warming world. *Scientific Reports*, *8*(1), 1576. https://doi.org/10.1038/s41598-018-19952-4

References From the Supporting Information

Ellison, S. & Williams, A. (2012). *Eurachem/CITAC guide: Quantifying uncertainty in analytical measurement* (3rd ed.). Eurachem/CITAC. https://doi.org/10.25607/OBP-952

Hood, E. M. (2010). Introduction to the collection of expert reports and guidelines. In (Eds), E. M. Hood, C. L. Sabine, & B. M. Sloyan. *The GO-SHIP repeat hydrography manual: A collection of expert reports and guidelines. Version 1* (p. 2). (IOCCP Report Number 14; ICPO Publication Series Number 134). https://doi.org/10.25607/OBP-1351

Lauvset, S. K., Lange, N., Tanhua, T., Bittig, H. C., Olsen, A., Kozyr, A., et al. (2022). GLODAPv2.2022: The latest version of the global interior ocean biogeochemical data product. *Earth System Science Data*, *14*(12), 5543–5572. https://doi.org/10.5194/essd-14-5543-2022

Sabine, C. L., Feely, R. A., Millero, F. J., Dickson, A. G., Langdon, C., Mecking, S., & Greeley, D. (2008). Decadal changes in Pacific carbon. *Journal of Geophysical Research*, *113*(C7), C07021. https://doi.org/10.1029/2007JC004577

Wallace, D. (1995). *Monitoring global ocean carbon inventories Ocean Obs. Syst. Dev. Panel* (Vol. 54). Texas A&M University.

Wanninkhof, R., Doney, S. C., Bullister, J. L., Levine, N. M., Warner, M., & Gruber, N. (2010). Detecting anthropogenic CO_2 changes in the interior Atlantic Ocean between 1989 and 2005. *Journal of Geophysical Research*, *115*(C11), C11028. https://doi.org/10.1029/2010JC006251